Journal of Sound and Vibration (2000) **237**(2), 181–202
doi:10.1006/jsvi.2000.2998, available online at http://www.idealibrary.com on IDEAL®

A HYBRID FINITE ELEMENT FORMULATION FOR MID-FREQUENCY ANALYSIS OF SYSTEMS WITH EXCITATION APPLIED ON SHORT MEMBERS

XI ZHAO AND NICKOLAS VLAHOPOULOS

Department of Naval Architecture and Marine Engineering, The University of Michigan, 2600 Draper Road, Ann Arbor, MI 48109-2145, *U.S.A.*

(*Received* 9 *August* 1999, *and in final form* 21 *February* 2000)

A hybrid finite element method for computing mid-frequency vibrations is presented. In the mid-frequency region a system is comprised by some members that contain several wavelengths and some members that contain a small number of wavelengths within their dimensions. The former are considered long members and they are modelled by the energy finite element analysis (EFEA). The latter are considered short and they are modelled by the finite element analysis (FEA). In this paper the excitation is considered to be applied on the short members. The hybrid formulation computes the response of the entire system. The characteristics of the long members affect the behavior of the short members and the amount of power flow between the members of the system. The resonant characteristics of the short members and the boundary conditions imposed by the long members determine the amount of input power into the system. The interaction between members is described by a set of equations between the FEA and the EFEA primary variables at the interfaces between long and short members. The equations for the short and the long members and the interface equations are solved simultaneously. A theoretical formulation and a numerical implementation for systems that contain one wave type is presented. Analytical solutions for several co-linear beam configurations are compared to numerical results produced by the hybrid finite element method. Good correlation is observed for all analyses.
© 2000 Academic Press

1. INTRODUCTION

The frequency spectrum where simulation methods can be utilized for vibration analysis can be divided into three regions: low, mid, and high frequency. The low-frequency region is defined as the frequency range where all components are short with respect to a wavelength (short members). Short members respond with low model density, and resonant effects are dominant. No uncertainties with respect to the natural frequencies or the dimensions of the short members are considered. Conventional finite element analysis (FEA) is a practical numerical approach for simulating low-frequency vibrations [1–3].

The high-frequency region is defined as the frequency range where all component members of a system are long with respect to a wavelength (long members). Statistical energy analysis (SEA) [4–8], and energy finite element analysis (EFEA) [9–15] can be used for vibro-acoustic simulations at high frequencies. SEA is an established approach for high-frequency analysis. EFEA constitutes a recent development for high-frequency analysis [9–15]. In EFEA, the primary variable is defined as the time- and space-averaged energy density (energy density). The governing differential equations are developed with respect to the energy density, and a finite element approach is employed for the numerical

0022-460X/00/420181 + 22 $35.00/0 © 2000 Academic Press

solution. Both SEA and EFEA provide meaningful results for the ensemble average response [16] when all the members in the system have high model density.

The mid-frequency region is defined as the frequency range where some of the components of a system are long and other members are short. In the mid-frequency range, the FEA method requires a prohibiting large number of elements to perform an analysis due to the presence of the long members. The formulations of the energy methods (SEA and EFEA) contain assumptions that are valid when all components of a system have high model density. Based on the condition of high model density, the SEA formulation considers the normal modes within a frequency band as equally spaced, containing the same amount of energy, and demonstrating an equal amount of damping [8]. The condition of a small wavelength with respect to the dimension of a member in the EFEA is equivalent to the condition of high model density in SEA. The requirement for small wavelength in the EFEA allows to neglect near-field effects in a wave equation during the development of the governing differential equation. Thus, the energy methods cannot capture resonant effects in the behavior of a system in the mid-frequencies. The resonant effects are generated from the presence of the short members.

In the energy methods, the amount of power transferred between members at joint is defined in terms of coupling loss factors (in SEA) or power transfer coefficients (in EFEA). Analytical solution of semi-infinite members are employed for defining the power transfer characteristics of each joint [17]. The computations are meaningful when the members connected at the joint are long. Then, the power transfer characteristics of the long members can be considered the same with the power transfer characteristics of the semi-infinite members. The requirement for high modal density is necessary because the information produced by the analytical solutions of the semi-infinite members captures the exchange of power flow between members when there is an equal amount of coupling between the normal modes of the members. If large differences exist in the power flow due to the distinct resonant behavior of the short members, then the power transfer characteristics cannot be identified properly from analytical solutions of semi-infinite members. In addition, the behavior of the short members cannot be computed correctly by the energy methods because of resonant effects that are important for the overall behavior of a short member are neglected in the current form of the energy methods.

In the past, conventional finite element models have been employed in order to determine the SEA coupling loss factors [18–23] or the EFEA power transfer coefficients [14] instead of employing analytical solutions of semi-infinite members. Specially, SEA coupling loss factors have been computed through finite element computations for assemblies of fully connected plates [18, 21], for beam junctions [19], for interfaces between structural and acoustic subsystems [22], for the sound transmission between walls in a building [20], and for connections between rods [23]. EFEA power transfer coefficients have been computed through finite element computations for spot-welded connections [14]. The rationale in all these developments is to employ conventional EFA for capturing the coupling mechanism when the connection between members presents a complexity that cannot be accounted by the analytical solutions of semi-infinite members. The approach of utilizing FEA for computing the power transfer characteristics is the only computational option for complex or discontinuous joints, and this approach provides an alternative to evaluating the power transfer characteristics through testing.

An approach based on creating a statistical Green kernel for a boundary element formulation for assembled rods and beams in the mid-frequency range has been presented [24]. The statistical Green kernel is constructed based on random mechanical constants. The fundamental solution is then considered as a random function. A direct boundary

element approach is employed to achieve numerical solution. Examples of analyzing a single rod, two co-linear rods, and a single beam were presented [24].

The concept of combining an FEA and an SEA formulation for developing a hybrid approach has been presented [25]. The lack of compatibility at the joint between the SEA variables and the FEA variables became a main issue. An optimization routine was developed to approximate the compatibility at the joint between the SEA and the FEA variables. Recently, another hybrid approach based on coupling FEA and SEA methods has been presented for rod elements [26]. The method was based on utilizing FEA to compute the low-frequency global modes of a system and SEA to represent the high-frequency local modes of each subsystem. The low-frequency global modal degrees of freedom were coupled to the high-frequency local modal degrees of freedom. Assumptions of weak coupling between local and global degrees of freedom, and rain-on-the-roof type of excitation were made. Also an implicit assumption was made that it was possible to readily identify the global and the local modes of a system. The validation was based on an example of two co-linear rod elements [26].

In a previous work, a fundamentally new formulation was presented for mid-frequency analysis [27]. It was based on coupling conventional FEA models of short members to EFEA models of long members. The excitation was considered to be applied on the long members only. The joints between long and short members were modelled by combining analytical solutions of semi-infinite members that represent the long members to FEA numerical models for the short members. Two sets of data were produced from the coupling process. The first set was comprised of power transfer coefficients for each EFEA member at a joint with a short member. The computed power transfer coefficients contained the effect of the resonant behavior of the short members and the damping that could be present in the short members. The second set of data was comprised of relationships between the primary variables of the EFEA model and the primary variables of the FEA model at a joint between long and short members. A major advantage offered from the wave-based formulation of the EFEA is the distinction between the energy (and the power) associated with waves travelling towards and away from a joint. At a joint between a long and a short member only the energy associated with the impinging wave contributes to the excitation of the short member. Thus, when multiple members are connected together, effects of strong coupling, power re-injection [16], indirect power flow [28], and power re-radiation [29] can be captured correctly by the hybrid finite element solution.

In this paper, the hybrid finite element formulation is significantly enhanced in order to consider the excitation applied on a short member. The coupling equations between long and short members must account for the excitation applied on a short member. The resonant and damping characteristics of the short members remain important for the overall behavior of the system and the response of the short members. The boundary conditions imposed by the adjacent long members are important for the response of the short members where the excitation is applied. The amount of power transferred from the short to the adjacent long members depends on the amount of energy eventually stored in the long members. For certain external excitation applied on a short member, the amount of input power in the system depends on the resonant characteristics of the short member and the boundary conditions imposed by the adjacent long members. In order to address these issues, a new hybrid FEA formulation for the joints between short and long members is developed. A system of interface equations between the FEA and EFEA primary variables is developed for capturing the relationship between the power transferred from the short to the long members and the energy which is stored within the long members. The interface equations are developed from compatibility and equilibrium conditions at the joint. An

iterative solution process is formulated for solving simultaneously the FEA system of equations, the EFEA system of equations, and the system of interface equations between short and long members. Theoretical developments and numerical implementation are presented for systems with one type of energy. Numerical solutions of the new hybrid FEA formulation are compared successfully to analytical solutions for several systems of co-linear beams. Good correlation is observed between numerical and analytical results.

2. MATHEMATICAL FORMULATION OF THE HYBRID FINITE ELEMENT ANALYSIS

The primary concept of the hybrid finite element formulation is to utilize low-frequency FEA models for deriving energy information for the short members, and to integrate them with EFEA models representing the long members. Due to the presence of the long members in the system, the response of all members will remain incoherent inasmuch as the short members will be subjected to an incoherent excitation at the points where they are connected to the long members. Previous work has demonstrated how low-frequency vibro-acoustic models can be analyzed when they are subjected to incoherent excitation [30, 31]. The EFEA is selected to be coupled with the low-frequency methods because it constitutes a wave approach for high-frequency solutions and it is based on a spatial discretization of the system that is being modelled. Thus, it is possible to develop appropriate interface conditions at the joints between the primary variables of the EFEA formulation and the primary variables of the FEA formulation since both can be associated with displacement properties at the joint.

2.1. BACKGROUND ONE EFEA AND HYBRID FEA FORMULATIONS

In EFEA, the energy density and the power flow constitute the primary variables of the formulation [9–13]. The energy density and the power flow are expressed in terms of a far-field displacement solution. One of the bending degree of freedom in a beam will be considered in this formulation. By time averaging over one period and space averaging over one wavelength, a relationship can be derived between the time- and space-average energy density and power flow, $\langle \underline{e} \rangle$ and $\langle \underline{q} \rangle$ respectively [13]:

$$\langle \underline{q} \rangle = \frac{-4c_b^2}{\eta\omega} \frac{\mathrm{d}\langle \underline{e} \rangle}{\mathrm{d}x}, \tag{1}$$

where η is the hysterisis damping factor, ω the radian frequency, and c_b the phase speed of bending waves. The time- and space-averaged dissipated power $\langle \underline{\Pi}_{diss} \rangle$ can be associated to the corresponding energy density [17],

$$\langle \underline{\Pi}_{diss} \rangle = \eta\omega \langle \underline{e} \rangle. \tag{2}$$

A power balance at the steady state results in [9, 11, 12]

$$\langle \underline{Q}_{in} \rangle = \langle \underline{\Pi}_{diss} \rangle + \frac{\mathrm{d}\langle \underline{q} \rangle}{\mathrm{d}x}, \tag{3}$$

where $\langle \underline{Q}_{in} \rangle$ = input power. Substituting equations (1) and (2) into equation (3) results in the governing differential equation for the time- and space-averaged energy density,

$$\frac{-c_g^2}{\eta\omega} \frac{\mathrm{d}^2\langle \underline{e} \rangle}{\mathrm{d}x^2} + \eta\omega\langle \underline{e} \rangle = \langle \underline{Q}_{in} \rangle, \tag{4}$$

where c_g is the group speed of the bending waves. A finite element approach is employed for solving equation (4) numerically, resulting in [32]

$$[E^e]_i \{e^e\}_i = \{F^e\}_i + \{Q^e\}_i, \tag{5}$$

where superscript "e" indicates element-based quantities, subscript "i" indicates the ith element, $\{e^e\}_i$ the vector of nodal values for the time- and space-averaged energy density for the ith element, $[E^e]_i$ the system matrix for the ith element, $\{F^e\}_i$ the vector of input power at the nodal locations of the ith element, and $\{Q^e\}_i$ the vector of power flow at the boundary locations of the ith element. In EFEA, the primary variables of the formulation are associated with energy density. However, the external excitation and the interface conditions between members are defined in terms of power input and power flow respectively. In EFEA, the term $\{Q^e\}_i$ provides the mechanism for connecting elements together across discontinuities [32]. In the hybrid FEA formulation presented in this paper, $\{Q^e\}_i$ provides the mechanism for prescribing the power flow from the short to the long members due to the excitation applied on the short members.

In EFEA, at positions where different members are connected, or at locations of discontinuities, the energy density is discontinuous. The corresponding boundary between the elements defines a joint location. Therefore, during the assembly of the global system the element matrices do not couple, and the values of the internal power flow at the common node do not overlap to cancel each other. Instead, they remain as variables on the right-hand side of the equation

$$\begin{bmatrix} [E^e]_i & \\ & [E^e]_j \end{bmatrix} \begin{Bmatrix} \{e^e\}_i \\ \{e^e\}_j \end{Bmatrix} = \begin{Bmatrix} \{F^e\}_i \\ \{F^e\}_j \end{Bmatrix} + \begin{Bmatrix} \{Q^e\}_i \\ \{Q^e\}_j \end{Bmatrix}. \tag{6}$$

A special procedure is used for assembling the element matrix into the global matrix equations [32]. A specialized joint element equation is developed to formulate the connection between the discontinuous primary variables at the joint. The values of the power flow at the inter-element nodes corresponding to the two adjacent elements are expressed in terms of the corresponding energy densities [32],

$$\begin{Bmatrix} Q^e_{ic} \\ Q^e_{jc} \end{Bmatrix} = [J]^i_j \begin{Bmatrix} e^e_{ic} \\ e^e_{jc} \end{Bmatrix}, \tag{7}$$

where subscript "c" indicates the common node between elements "i" and "j", and $[J]^i_j$ is the joint matrix expressing the mechanism of power transfer between elements "i" and "j". The coefficients of the joint matrix are computed by power transfer coefficients derived from analytical solutions of semi-infinite members fully connected to each other, and by taking into account the continuity of the power flow across the joint. Introducing equation (7) into equation (6) results in

$$\left(\begin{bmatrix} [E^e]_i & \\ & [E^e]_j \end{bmatrix} + [JC]^i_j \right) \begin{Bmatrix} \{e^e\}_i \\ \{e^e\}_j \end{Bmatrix} = \begin{Bmatrix} \{F^e\}_i \\ \{F^e\}_j \end{Bmatrix}, \tag{8}$$

where $[JC]^i_j$ is the matrix comprising the coefficients of $[J]^i_j$ positioned in the appropriate locations.

In the mid-frequency range, a system is comprised of both long and short members. A hybrid FEA formulation has been presented for mid-frequency computations when the

external excitation is applied on long members of the system [27]. A FEA model for the short member is coupled with analytical solutions of semi-infinite members in order to formulate a hybrid joint. Power transfer coefficients and relationships between EFEA and FEA primary variables are computed by the hybrid joint formulation. The EFEA power transfer coefficients derived from a hybrid joint contain information about the dissipative and resonant characteristics of the short member. They are utilized for evaluating the terms of the joint matrix $[JC]_j^i$ for long members that are connected to short ones. The external excitation is considered applied on long members and the EFEA solution for the distribution of the energy density over all the long members is computed. The influence of the short members to the response of the long members is captured due to the derivation of the power transfer coefficients from the hybrid joint formulation. From the EFEA solution, the energy density associated with the waves impinging on the short members is computed. The relationships between the EFEA and FEA primary variables developed by the hybrid joint are employed for defining the excitation exerted on the short members. Because of the wave-based approach of the EFEA formulation, the amount of energy associated with the wave impinging on the short member can be identified from the energy density that constitutes the primary variable of the EFEA formulation. Only the energy associated with the impinging wave is employed for defining the excitation exerted on a short member. Thus, it is possible to account for power re-injection and power re-radiation effects when multiple long members are present in the system. The boundary conditions imposed by multiple long members connected to a short member are treated as incoherent since they originate from the reverberant fields that exist within each one of the long members. The response of the short members is evaluated after the EFEA computation for the long members has been completed.

2.2. HYBRID FEA FORMULATION FOR EXCITATION APPLIED ON SHORT MEMBERS

In this paper, the excitation is considered to be applied on a short member. The resonant, damping, and dissipative characteristics of the short members impact their own response as well as the behavior of the long members. The amount of power flow from the short to the adjacent long members and the response of the short members depend on the rigidity of the long members, the excitation applied on the short members, and the amount of energy stored in the long members. The amount of input power into a system depends on the resonant characteristics of the short members and the boundary conditions imposed by the adjacent long members. The interactions between the members must be taken into account during the solution process. A special iterative solution scheme is developed in order to address these considerations. In the new solution process, the behavior of the short and long members is computed simultaneously. The overall hybrid finite element formulation can be divided into two parts, the formulation of the hybrid FEA equations and the solution process. The former is divided into three stages: (1) The FEA system of equations for the short members are condensed to the degrees of freedom at the joint locations. The final condensed FEA system of equations includes the effect of the external excitation applied on short members. (2) The EFEA system of equations for the long members is developed. The power flow from the short members constitutes the internal power flow at joints between short and long members. (3) The joints between the short and long members are considered to have similar behavior with joints between short and semi-infinite members. Analytical solutions of semi-infinite members are coupled to the FEA models of the short members. A system of interface equations between the short and long members is formulated through continuity and equilibrium conditions at the interfaces between the short and long

members. The second part is comprised of the iterative solution process for the overall system. The three systems of equations, namely, the condensed FEA, the EFEA, and the interface equations, are solved simultaneously in order to account for the interactions between the members. The power flow from the short to the long members depends on the energy level in the long members and it is updated within each iteration. The final converged values of power flow are used for evaluating the energy distribution over all of the long members. At the same time the response of the short members is computed. It depends on the external excitation applied on the short members, the characteristics of the short members, and the boundary conditions imposed on the short members by the adjacent long members.

A finite element discretization is utilized for modelling each short members. The equation of motion can be written in matrix form as

$$[-\omega^2[M] + \mathrm{i}\omega[C] + [K]]\{u\} = \{R\} + \{F_I\} \Rightarrow [ST]\{u\} = \{R\} + \{F_I\}, \tag{9}$$

where $[M]$, $[C]$, $[K]$ are the mass, damping, and stiffness matrix respectively, $\{u\}$ is the displacement of vibration, $[ST]$ the global structural system matrix including the mass, damping, and stiffness effects, $\{R\}$ the vector of forces and moments imposed by external excitation or supports, and $\{F_I\}$ the vector of internal forces applied at the boundaries of the short member by the adjacent long members. Equation (9) can be partitioned into the degree of freedom at the interfaces with the long members and the remaining degrees of freedom. Since the current development considers one wave type in each member, the maximum number of long members connected to a short member is two. Therefore, the equations of the hybrid joint formulation are presented for the case of two long members connected to a short member. The FEA method is employed to model the short members. Several of them can be connected to each other and placed in between long ones. There is no inherent limitation in extending the developed concept to members with multiple wave types. Partitioning equation (9) for a short member results in

$$\begin{bmatrix} [ST_{11}] & [ST_{12}] \\ [ST_{21}] & [ST_{22}] \end{bmatrix} \begin{Bmatrix} u_m \\ \dfrac{\mathrm{d}u_m}{\mathrm{d}x} \\ u_n \\ \dfrac{\mathrm{d}u_n}{\mathrm{d}x} \\ \{u_2\} \end{Bmatrix} = \begin{Bmatrix} 0 \\ 0 \\ 0 \\ 0 \\ \{R_2\} \end{Bmatrix} + \begin{Bmatrix} F_m \\ M_m \\ F_n \\ M_n \\ \{0\} \end{Bmatrix}, \tag{10}$$

where subscript "m" corresponds to the displacement u_m and its derivative $\mathrm{d}u_m/\mathrm{d}x$ at the left joint with a long member, subscript "n" corresponds to the displacement u_n and its derivative $\mathrm{d}u_n/\mathrm{d}x$ at the right joint with a long member. F_m, M_m, F_n, M_n are the internal forces and moments exerted from the long members on the short members at the two joint locations, subscript "1" corresponds to the FEA degrees of freedom at the joints, subscript "2" corresponds to the remaining FEA degrees of freedom, and $\{R_2\}$ the forces and moments applied by external excitation or supports on the FEA degrees of freedom at any location other than the joints. From the lower part of equation (10), $\{u_2\}$ can be expressed in terms of

the FEA degrees of freedom at the joints and then substituted in the upper part. The condensation operation results in

$$[S]\begin{Bmatrix} u_m \\ \dfrac{\mathrm{d}u_m}{\mathrm{d}x} \\ u_n \\ \dfrac{\mathrm{d}u_n}{\mathrm{d}x} \end{Bmatrix} = \begin{Bmatrix} F_m \\ M_n \\ F_n \\ M_n \end{Bmatrix} + \begin{Bmatrix} F_{Rm} \\ M_{Rm} \\ F_{Rn} \\ M_{Rn} \end{Bmatrix}, \tag{11}$$

where $[S] = [[ST_{11}] - [ST_{12}][ST_{22}]^{-1}[ST_{21}]]$ is the condensed FEA system of equations, and

$$\begin{Bmatrix} F_{Rm} \\ M_{Rm} \\ F_{Rn} \\ M_{Rn} \end{Bmatrix} = -[ST_{12}][ST_{22}]^{-1}\{R_2\}$$

is the vector of condensed external forces and moments applied on the short members.

The interaction forces and moments F_m, M_m, F_n, M_n between the long and the short members at the two joints can be expressed in terms of the primary variables of the FEA formulation at the joints and the entries of matrix $[S]$ as well as the condensed forces and moments, F_{Rm}, M_{Rm}, F_{Rn} and M_{Rn}:

$$\begin{aligned} S_{11}u_m + S_{12}\frac{\mathrm{d}u_m}{\mathrm{d}x} + S_{13}u_n + S_{14}\frac{\mathrm{d}u_n}{\mathrm{d}x} - F_{Rm} &= F_m, \\ S_{21}u_m + S_{22}\frac{\mathrm{d}u_m}{\mathrm{d}x} + S_{23}u_n + S_{24}\frac{\mathrm{d}u_n}{\mathrm{d}x} - M_{Rm} &= M_m, \\ S_{31}u_m + S_{32}\frac{\mathrm{d}u_m}{\mathrm{d}x} + S_{33}u_n + S_{34}\frac{\mathrm{d}u_n}{\mathrm{d}x} - F_{Rn} &= F_n, \\ S_{41}u_m + S_{42}\frac{\mathrm{d}u_m}{\mathrm{d}x} + S_{43}u_n + S_{44}\frac{\mathrm{d}u_n}{\mathrm{d}x} - M_{Rn} &= M_n, \end{aligned} \tag{12}$$

where S_{ij} is the entire in the ith row and jth column of matrix $[S]$. The system of equation (12) constitutes the foundation for deriving the system of compatibility equations at the interfaces between the short and long members.

The joints between the short and long members are modelled by analytical solutions of semi-infinite members coupled to the FEA model of the short member. The FEA model includes any damping characteristics present in the short member. Waves are considered to impinge on the short member from both the left and the right semi-infinite members. A farfield term for an impinging right travelling wave, and both a near and a farfield term for a reflected/transmitted left travelling wave are present in the analytical expression of the left semi-infinite member:

$$W_m(x_m, t) = w_m(x_m)\,\mathrm{e}^{\mathrm{i}\omega t} = (A_m\mathrm{e}^{-\mathrm{i}k_m x_m} + C_m\mathrm{e}^{\mathrm{i}k_m x_m} + D_m\mathrm{e}^{k_m x_m})\,\mathrm{e}^{\mathrm{i}\omega t}. \tag{13}$$

The expression of the right semi-infinite member contains a farfield term for an impinging left travelling wave, and both near and farfield terms for the reflected/transmitted right travelling wave:

$$W_n(x_n, t) = w_n(x_n)\,\mathrm{e}^{\mathrm{i}\omega t} = (A_n \mathrm{e}^{-\mathrm{i}k_n x_n} + B_n \mathrm{e}^{-k_n x_n} + C_n \mathrm{e}^{\mathrm{i}k_n x_n})\,\mathrm{e}^{\mathrm{i}\omega t}, \tag{14}$$

where subscripts "m" and "n" indicate the left and right semi-infinite members respectively, A ,B are the amplitudes of far and nearfield components of a right travelling wave, respectively, and C, D the amplitudes of far and nearfield components of a left travelling wave. The wave numbers can be obtained by the equations

$$k_m = \left[\frac{\omega^2 \rho_m S_m}{E_m I_m}\right]^{1/4}, \qquad k_n = \left[\frac{\omega^2 \rho_n S_n}{E_n I_n}\right]^{1/4}, \tag{15, 16}$$

where ρ is the density, S the cross-sectional area, EI the bending rigidity.

The terms A_m and C_n are associated with the two impinging waves. Their presence is important for the iterative solution process because A_m and C_n are related to the energy level in the two long members. The amount of power flow from a short member to the adjacent long members depends on the energy level in the long members. As it will be discussed later in the iterative solution section, the amount of power flow from the short to the long members is updated within each iteration by updating from the EFEA solution the terms A_m and C_n that correspond to the impinging waves.

Continuity of displacement and slope and equilibrium of force and moment at the interfaces between the short and long members are expressed in terms of the displacements and the slopes at the two ends of the short beam, u_m, $\mathrm{d}u_m/\mathrm{d}x$, u_n and $\mathrm{d}u_n/\mathrm{d}x$, and the coefficients of the semi-infinite members A_m, C_m, D_m, A_n, B_n and C_n. The continuity conditions for the displacement and the slope, and the equilibrium of force and moment at the joints between the short and the semi-infinite members result in a system of eight equations between the primary variables of the FEA formulation, u_m, $\mathrm{d}u_m/\mathrm{d}x$, u_n and $\mathrm{d}u_n/\mathrm{d}x$, and the coefficients of the analytical wave expressions of the semi-infinite members. The system of equations can be expressed in matrix form as

$$\begin{bmatrix}
1 & 0 & 0 & 0 & -1 & -1 & 0 & 0 \\
0 & -1 & 0 & 0 & \mathrm{i}k_m & k_m & 0 & 0 \\
0 & 0 & 1 & 0 & 0 & 0 & -1 & -1 \\
0 & 0 & 0 & 1 & 0 & 0 & \mathrm{i}k_n & k_n \\
S_{11} & S_{12} & S_{13} & S_{14} & \mathrm{i}(EI)_m k_m^3 & -(EI)_m k_m^3 & 0 & 0 \\
S_{21} & S_{22} & S_{23} & S_{24} & -(EI)_m k_m^2 & (EI)_m k_m^2 & 0 & 0 \\
S_{31} & S_{32} & S_{33} & S_{34} & 0 & 0 & \mathrm{i}(EI)_n k_n^3 & -(EI)_n k_n^3 \\
S_{41} & S_{42} & S_{43} & S_{44} & 0 & 0 & (EI)_n k_n^2 & -(EI)_n k_n^2
\end{bmatrix}
\begin{Bmatrix}
u_m \\ \dfrac{\mathrm{d}u_m}{\mathrm{d}x} \\ u_n \\ \dfrac{\mathrm{d}u_n}{\mathrm{d}x} \\ C_m \\ D_m \\ A_n \\ B_n
\end{Bmatrix}$$

$$= \begin{Bmatrix} 1 \\ \mathrm{i}k_m \\ 0 \\ 0 \\ \mathrm{i}(EI)_m k_m^3 \\ (EI)_m k_m^2 \\ 0 \\ 0 \end{Bmatrix} A_m + \begin{Bmatrix} 0 \\ 0 \\ 1 \\ \mathrm{i}k_n \\ 0 \\ 0 \\ \mathrm{i}(EI)_n k_n^3 \\ -(EI)_n k_n^2 \end{Bmatrix} C_n + \begin{Bmatrix} 0 \\ 0 \\ 0 \\ 0 \\ F_{Rm} \\ M_{Rm} \\ F_{Rn} \\ M_{Rn} \end{Bmatrix}. \tag{17}$$

The four FEA variables at the interfaces and the four coefficients associated with the reflected/transmitted waves constitute the unknown variables. The condensed external forces of the FEA formulation and the coefficients associated with the impinging waves constitute the excitation. The impinging waves are related directly to the energy stored in the long members. By solving the system of equation (17), each one of the eight unknowns can be computed in terms of the amplitudes of the impinging waves A_m and C_n, and the external excitation applied on the short beam.

The coefficients C_m and A_n are related to the farfield reflected/transmitted waves. The amount of farfield power flowing from the short to the left (q_m) and right (q_n) long members is associated with both the impinging waves and the farfield reflected/transmitted waves and can be computed from A_m, C_m and A_n, C_n respectively.

$$q_m = -(EI)_m k_m^3 \omega(|A_m|^2 - |C_m|^2), \qquad q_n = (EI)_n k_n^3 \omega(|A_n|^2 - |C_n|^2). \tag{18}$$

Right travelling power flow is defined as positive. Because q_m is a left travelling power, the minus sign outside the parenthesis makes q_m a positive quantity. Once q_m and q_n are evaluated, they can be used to define the internal power flow at the interface nodes of the long members with the short ones in the EFEA system of equations. In order to expedite the computations, a unit power input is considered to be applied at the joint of each long member with a short member and the resulting energy densities at the joint are computed once ($\overline{e_m}$ for the left member, $\overline{e_n}$ for the right member). Equation (6) is employed for computing the EFEA solution for each long member. Then the energy densities corresponding to the power flow q_m and q_n that is computed from equation (18) can be evaluated:

$$e_m = \overline{e_m} q_m, \qquad e_n = \overline{e_n} q_n. \tag{19}$$

In this manner, the EFEA systems of equations for the long member need to be solved only once within the iterative solution process.

The energy density of the long members at the interfaces between the short and long members e_m and e_n are used to calculate the energy density e_m^+ and e_n^- associated with the waves impinging at the joint. The energy density at the edge of the left long member at the joint can be written as

$$e_m = e_m^+ + e_m^-. \tag{20}$$

The corresponding power flow is

$$q_m = -(q_m^+ - q_m^-) = -c_{gm} S_m (e_m^+ - e_m^-), \tag{21}$$

where q_m^+ and q_m^- are the absolute values of power flow associated with the right and left travelling waves in the left long member at the joint location, c_{gm} is the group speed of left long member m and S_m the cross-sectional area of long member m. The reason for the presence of the minus sign outside the parenthesis is the same as in the first equation of equation (18).

By solving equations (20) and (21), an expression can be obtained for e_m^+:

$$e_m^+ = \frac{e_m}{2} - \frac{q_m}{2c_{gm}S_m} = \left(\frac{\overline{e_m}}{2} - \frac{1}{2c_{gm}S_m}\right) q_m. \tag{22}$$

Similarly, e_n^- is expressed in terms of e_n and q_n, or $\overline{e_n}$ and q_n:

$$\begin{cases} e_n = e_n^+ + e_n^- \\ q_n = q_n^+ - q_n^- = c_{gn}S_n(e_n^+ - e_n^-) \end{cases} \Rightarrow e_n^- = \frac{e_n}{2} - \frac{q_n}{2c_{gn}S_n} = \left(\frac{\overline{e_n}}{2} - \frac{1}{2c_{gn}S_n}\right) q_n. \tag{23}$$

The values for e_m and e_n are from equation (19). The values for q_m and q_n are the internal power flow boundary conditions that are imposed as excitation on the EFEA system of equations. The energy density e_m^+ of the impinging wave from the left semi-infinite member is related to the amplitude of the right travelling wave by the equation

$$e_m^+ = \tfrac{1}{2}\rho_m\omega^2|A_m|^2. \tag{24}$$

In a similar manner, the energy density e_n^- of the impinging wave from the right semi-infinite member is related to the amplitude of the left travelling wave by the equation

$$e_n^- = \tfrac{1}{2}\rho_n\omega^2|C_n|^2. \tag{25}$$

$|A_m|$ and $|C_n|$ are calculated by equations (24) and (25) and constitute the updated amplitudes of the waves impinging from the two semi-infinite members within each iteration.

In the hybrid finite element formulation presented in this paper, three sets of equations have been developed: (1) FEA system for the short members, equation (12); (2) a relationship between power input from short to long members and the corresponding energy density at the joint, equation (19); (3) system of compatibility equations at the interfaces between short and long members, equation (17). These three systems of equations describe the behavior of each member and the interaction between the members. When the excitation is applied on a short member the amount of power flow to the adjacent long members depends on the characteristics of the short and the long members, the external excitation, the response of the short member, and the energy level in the long members. The energy level in the long members in turn depends on the amount of power flow from the short to the long members. The input power in the system depends on the resonant characteristics of the short member and the boundary conditions applied by the adjacent long members. Thus, the three sets of equations must be solved simultaneously and an iterative solution process has been developed.

At the beginning of the iterative solution initial values of $|A_m|$ and $|C_n|$ are defined. A_m and C_m represent the impinging waves from the long members. Two separate loops are developed for varying the phase angles associated with A_m and C_n in order to account for a large number of possible phase combinations. Introducing variation in the phase of the impinging waves is necessary in order to simulate the incoherent nature of the excitation applied by the long members on the short. One of the exterior excitation forces applied on the short member is considered to have the zero reference phase. The phase angles of A_m and C_n (ϕ_{A_m} and ϕ_{C_n}) vary between zero to 2π at a constant increment separately. The FEA

primary variables u_m, $\mathrm{d}u_m/\mathrm{d}x$, u_n, $\mathrm{d}u_n/\mathrm{d}x$ at the joints, and the unknown wave coefficients C_m, D_m, A_n, B_n associated with the reflected/transmitted waves in the long members are computed by equation (26). Solutions to equation (26) are computed for each specific pair of ϕ_{A_m} and ϕ_{C_n}. The total input power into the system and the power flow from the short to the long members q_m and q_n are evaluated at the completion of the loops associated with the variation of the phase. The computations are based on energy-based summations since the behavior of the long members is considered to be incoherent.

The energy density of the long members at the joints is evaluated from the values of the internal power flow at the joints q_m and q_n, equation (19). The response, the resonant, and the damping characteristics of the short members determine the power flow to the long members and affect the distribution of the energy density on the long members. The distribution of the energy density over all of the long members is evaluated. Equations (22)–(25) are employed for computing amplitudes $|A_m|$ and $|C_n|$ of the waves impinging from the long members to the short at the joint locations. The new values are compared with the old ones for convergence. The iterative process continues until the convergence criterion is satisfied. During the iterative process only the interface FEA degrees of freedom are evaluated within each iteration. For computational efficiency, the entire response of the short and the long members is computed only after convergence has been achieved. For each phase combination (ϕ_{A_m} and ϕ_{C_n}) of the impinging waves the converged values of $|A_m|$, $|C_n|$, u_m, $\mathrm{d}u_m/\mathrm{d}x$, u_n, $\mathrm{d}u_n/\mathrm{d}x$ are utilized along with equations (10), (12) and (17) to compute the behavior of the short members. The response of the short members is the result of the external excitation applied on them and the incoherent boundary conditions applied by the adjacent long members. The behavior of the short members is computed by adding

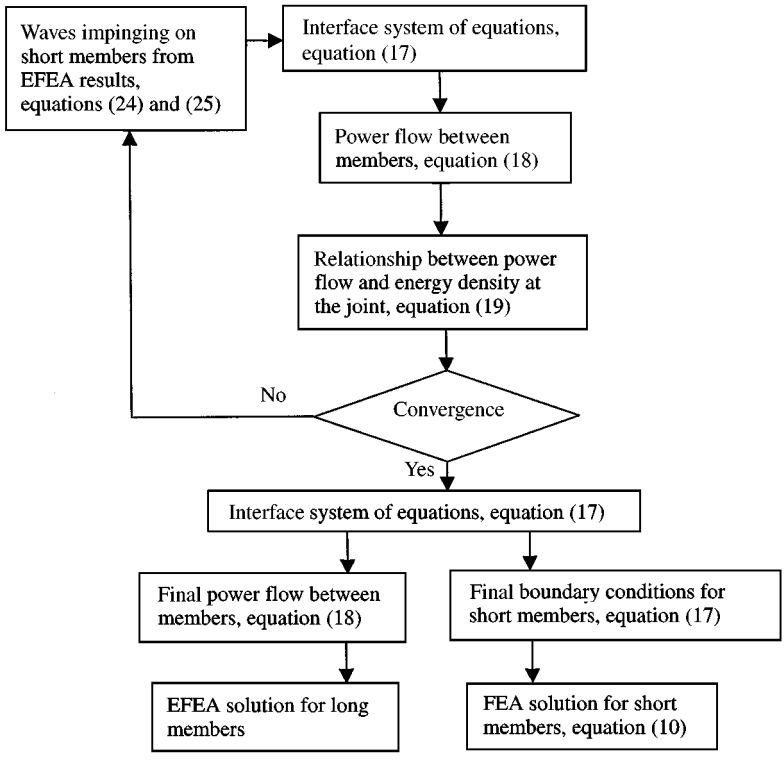

Figure 1. Flow chart of the iterative solution process.

on an energy basis the response of the short members computed at each phase combination of impinging waves. Figure 1 presents a flow chart of the iterative solution process.

3. VALIDATION

The validity of the basic research presented in this paper is demonstrated by computing the flexural energy of several systems comprised by long and short co-linear beam members and comparing the numerical results to analytical solutions. Some beams contain six or more flexural wavelengths and constitute long members while other beams contain a smaller number of wavelengths and constitute short members. Two main configurations (Table 1) of a three-beam systems (Figure 2) are analyzed. The three-beam system is comprised of two long beams inter-connected by a short one. Free end boundary conditions are considered for the two ends of the long beams that are not attached to the short members. Excitation is applied on the short beam. In some analyses, the excitation is applied at the center of the short beam and the results are expected to be symmetric with respect to the center of the system. In other cases, two excitation forces with 180° phase difference are applied on the short member. This type of excitation is employed for demonstrating that hybrid method can account for phase relationships of multiple excitations applied on a short member. The hybrid results are compared to analytical solutions. A solution obtained by the EFEA method is also presented in the results in order to demonstrate the inability of a high-frequency formulation to perform computations in the mid-frequency range. In the analytical and in the hybrid solutions the external force is prescribed as excitation. In the EFEA the driving point admittance is utilized to define an approximate power input into the system. Utilization of the driving point admittance is a typical approach for defining the excitation in energy methods [8].

TABLE 1

Properties of beams employed in the validation

		Long beam	Short beam
Young's modulus of elasticity E (N/m^2)		$19{\cdot}5 \times 10^{10}$	$19{\cdot}5 \times 10^{10}$
Moment of inertia I (m^4)		$9{\cdot}365 \times 10^{-10}$	$5{\cdot}853 \times 10^{-11}$
Mass density ρ (kg/m^3)		7,700	7,700
Damping factor η		0·02	0·02
Cross-sectional area A (m^2)		$1{\cdot}935 \times 10^{-4}$	$0{\cdot}4839 \times 10^{-4}$
Cross-sectional dimensions width × height (m)		0·0254 × 0·00762	0·0127 × 0·00381
Length of members (m)	System 1	3	1
	System 2	6	1

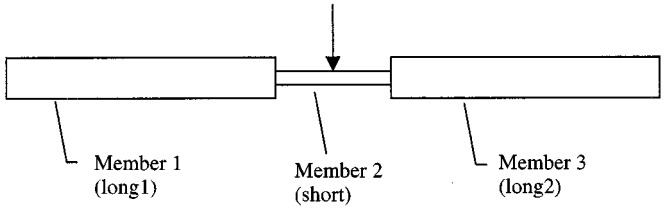

Figure 2. Three-beam assembly utilized in the validation.

In order to simulate the ensemble average behavior of the long members in the analytical solution, a 4% variation is introduced in the length of the long members [33]. The ensemble of systems incorporates all the effects of uncertainty associated with the long members but it is defined for a specific frequency [16]. In the validation presented here it is preferred to introduce the uncertainty associated with the long members through an ensemble of systems rather than frequency averaging in order to better demonstrate in the solution the highly resonant effects of the short member. The cross-sectional properties of the long and the short members are the same with the values used in previous validation studies [27] and they are also summarized in Table 1. In the selected configuration, the short member has lower bending rigidity than the long members. Therefore, it is expected that the behavior of the short member will depend strongly on the response of the long members. The selected bending rigidities will test the hybrid formulation for capturing properly the interaction between long and short members. The selected configurations also demonstrate that the characterization of a member as long or short depends on both the bending rigidity and its length. In the configurations selected for the validation the wavelength in the short member is smaller than the wavelength in the long members; however, the lengths of the beams become the determining factor of quantifying them as long or short.

3.1. ANALYSIS OF CO-LINEAR BEAM SYSTEMS

Results computed by the hybrid FEA method for System 1 are compared with analytical solutions (see Appendix A) and the EFEA. Analysis is first performed in the frequency range 440–605 Hz. An external excitation force equal to 1 N is the same for the analytical and the hybrid FEA. The corresponding input power for the EFEA is computed form the driving point admittance. Results for the total energy in the system are presented in Figure 3(a). The same force is specified as excitation; therefore, it is expected for the analytical and the hybrid solutions to demonstrate the same amount of total energy at each frequency, since the total energy of the system is proportional to the input power. The good agreement between the two solutions observed in Figure 3 validates that the hybrid FEA captures correctly the input power for a certain external excitation, the power balance between members, and the modeling of energy dissipation. The EFEA results are typical of high-frequency solutions since they cannot capture the variation of input power due to the resonant characteristics of the system. The averaged energy density for one of the long and short members are presented in Figure 3(b) and Figure 3(c), respectively. Since the system and the excitation are symmetric, the response of the two long members is exactly the same, as expected, and results are presented for only one of two long members. There is good agreement between the hybrid and the analytical solutions for all the members throughout the frequency range. The resonant characteristics of the system are accounted and the magnitude of the response correlates well at all frequencies. Results for the distribution of the space-averaged energy density over each member are presented in Figure 4 for the resonant frequency of 495 Hz. The hybrid formulation captures correctly the power transfer mechanism between members since it accounts properly for resonant effects, energy dissipation, power balance and power re-injection. The good correlation observed between the hybrid and the analytical solutions for System 1 demonstrates that the system of coupling equations between the long and short members calculates properly the amount of input power corresponding to the excitation applied on the short member. Finally, the iterative solution scheme that accounts for the relationship between power flow from short to long members and energy stored in the long members is also validated by the correlation.

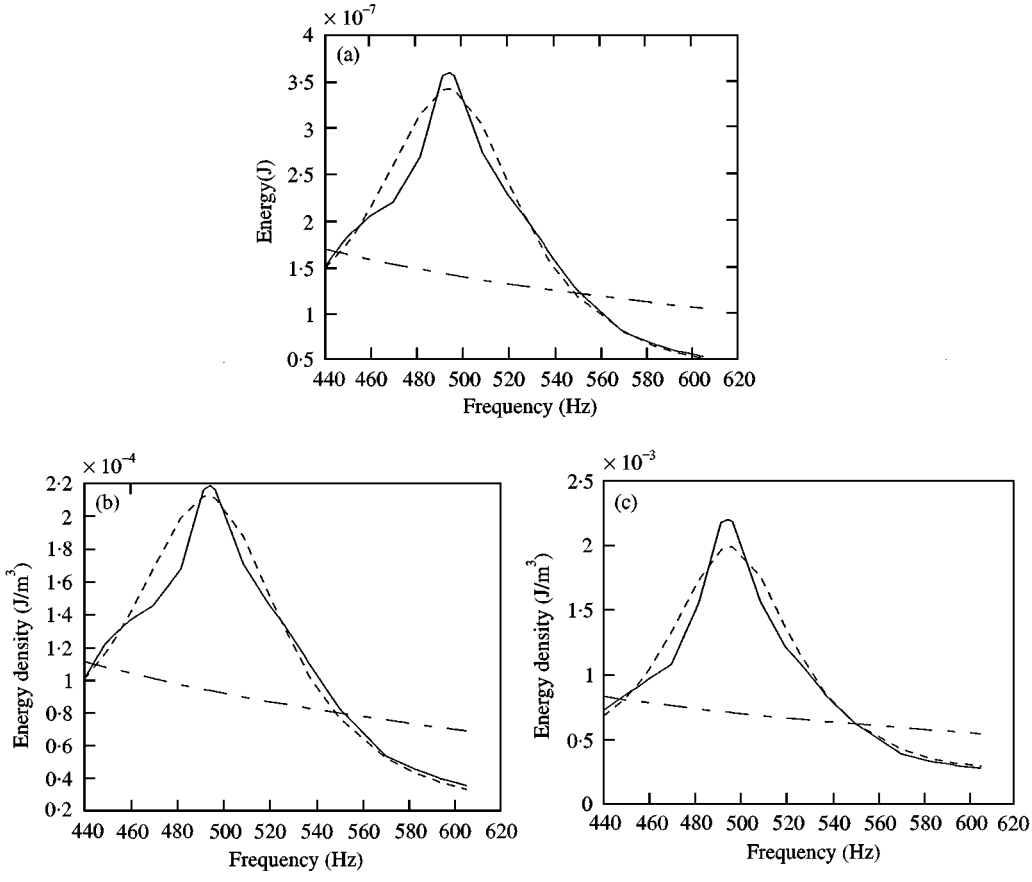

Figure 3. Analytical, hybrid, and EFEA results for System 1, 440–605 Hz: ———, analytical; - - -, hybrid; - · - · - ·, EFEA. (a) Total energy for the system; (b) space-averaged energy density for the left long beam; (c) space-averaged energy density for the short beam.

In order to demonstrate that the hybrid solution can account for relative phase information between multiple excitations applied on a short member the excitation applied on the short beam is altered. Two forces of 1 N each are applied at locations one-third length away from the edges of the short member. The two forces have 180° phase difference. An analytical solution is computed and results are compared with the hybrid FEA. A high-frequency EFEA solution is also presented with input power determined from the driving point admittance. Results for the total energy in the system are presented in Figure 5(a) over the frequency range 560–760 Hz. Good correlation is observed for the total energy stored in the system and the external power input. Resonant behavior is observed at different frequencies compared with Figure 3(a) because the non-symmetric modes are primarily excited this time. Results for the averaged energy density for the left long and the short members are presented in Figure 5(b) and 5(c) respectively. The distribution of the space-averaged energy density over each member for the resonant frequency of 642 Hz is presented in Figure 6. Good correlation between the analytical and hybrid solutions is observed in all the results. As expected, the high-frequency solution provided by the EFEA severely underpredicts the resonant response of the system, since the input power is approximated by the driving point admittance of infinite members [8, 22].

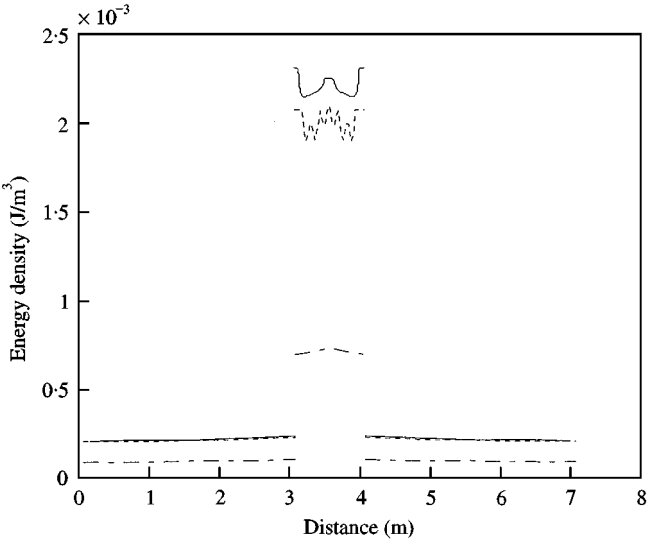

Figure 4. Analytical, hybrid, and EFEA results for the space-averaged energy density in System 1, 495 Hz: ———, analytical; ----, hybrid; - · - · - ·, EFEA.

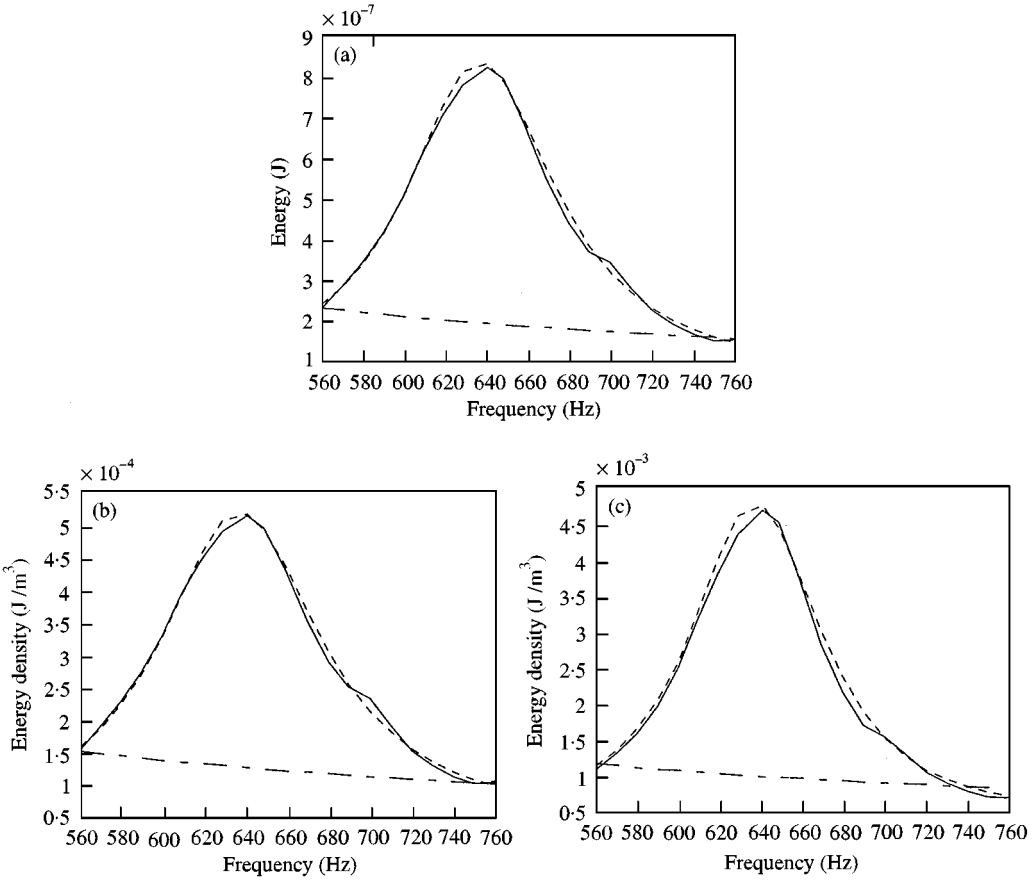

Figure 5. Analytical, hybrid, and EFEA results for System 1 with altered excitation, 560–760 Hz: ———, analytical; ----, hybrid; - · - · - ·, EFEA. (a) Total energy for the system; (b) space-averaged energy density for the left long beam; (c) space-averaged energy density for the short beam.

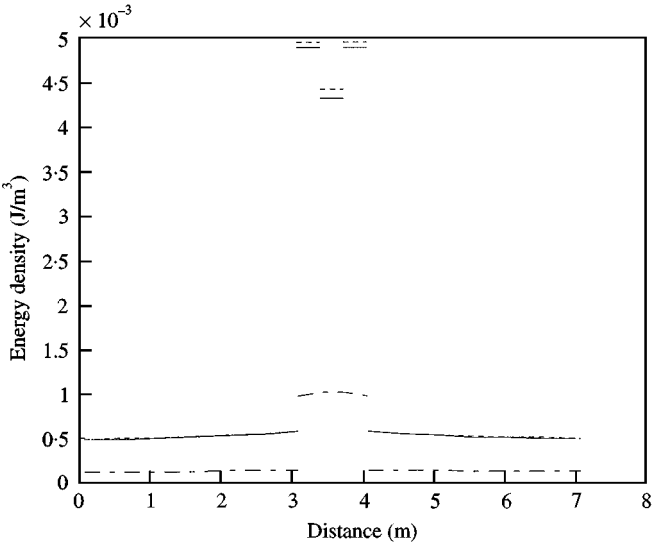

Figure 6. Analytical, hybrid, and EFEA results for the space-averaged energy density in System 1 with altered excitation, 642 Hz: ———, analytical; ----, hybrid; - · - · - ·, EFEA.

Hybrid and analytical solutions for System 2 are presented in a manner similar to System 1. The good correlation between the two solutions is retained. Compared with System 1, the long members in System 2 are extended from 3 to 6 m. The modification in the length alters the boundary conditions between the three members. The total energy in the system is presented in Figure 7(a) for the frequency range 440–605 Hz. The results between the analytical and the hybrid FEA solutions correlate well. The EFEA underpredicts the amount of input power in the system. The hybrid results for the two long members are identical, as expected, due to symmetry. The averaged energy density for one of the long members and the short member are presented in Figure 7(b) and 7(c) respectively. Results for the distribution of the space-averaged energy density over each member are presented in Figure 8 for the resonant frequency of 495 Hz. The good correlation between the hybrid and the analytical solutions validates that the hybrid formulation captures correctly the input power and the power transfer mechanism between the three members in the system.

The presence of the long members in the system influences the results in two ways; by imposing certain rigidity boundary conditions and by limiting the amount of power flow from the short member to the long members. The latter occurs due to the waves reflected from the boundaries of the long member that impinge back on the joint (power re-injection). In order to demonstrate the influence of power re-injection in the behavior of the system results for System 2 are compared with an analytical solution of the short member connected to two semi-infinite members. It is demonstrated that if the long members are represented as semi-infinite, the power re-injection effect is eliminated and error is introduced in the response of the short member. The same external force is applied on the two systems. Results for the averaged energy density in the short member are presented in Figure 9(a) for the frequency range 440–605 Hz. The amount of energy computed by the hybrid solution is consistently higher than the amount of energy predicted by the semi-infinite solution. This is expected since in reality power is reinjected back to the short member from the long members. Power re-injection is captured correctly by the hybrid FEA. Results for the distribution of the space-averaged energy density over each member are presented in Figure 9(b) for the resonant frequency of 495 Hz. It can be seen that if

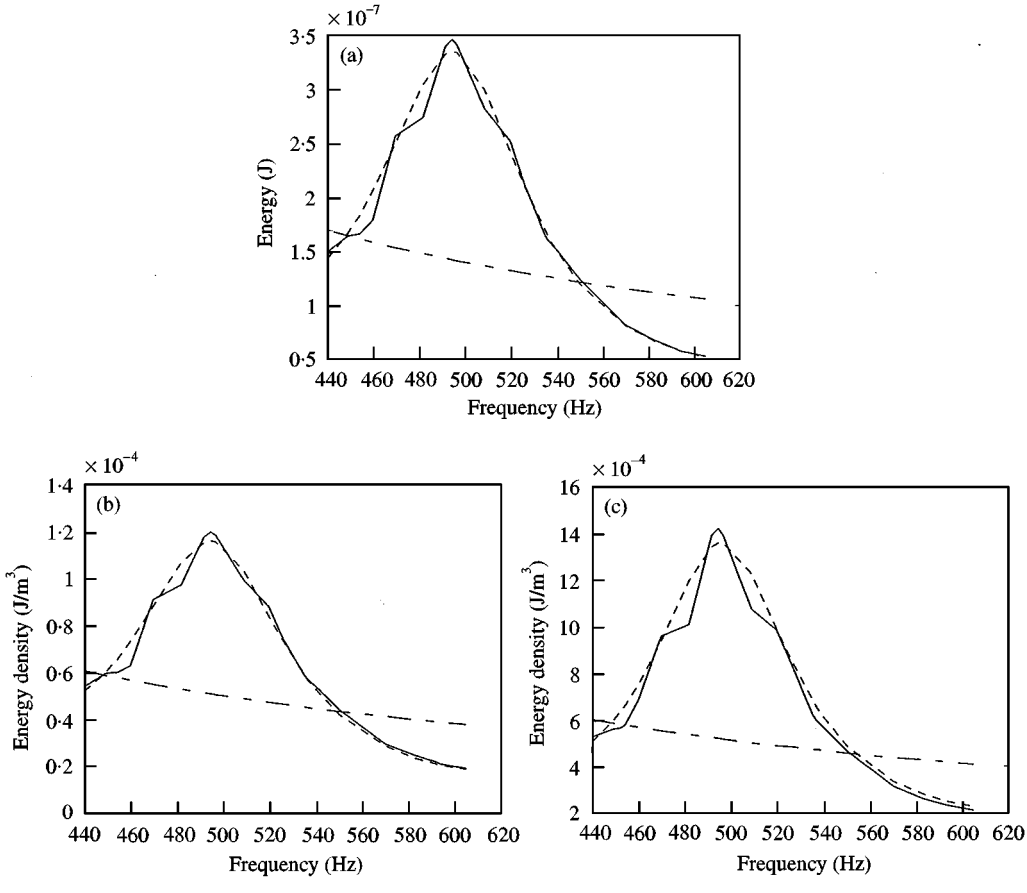

Figure 7. Analytical, hybrid, and EFEA results for System 2, 440–605 Hz: ———, analytical; ----, hybrid; - · - · - ·, EFEA. (a) Total energy for the system; (b) space-averaged energy density for the left long beam; (c) space-averaged energy density for the short beam.

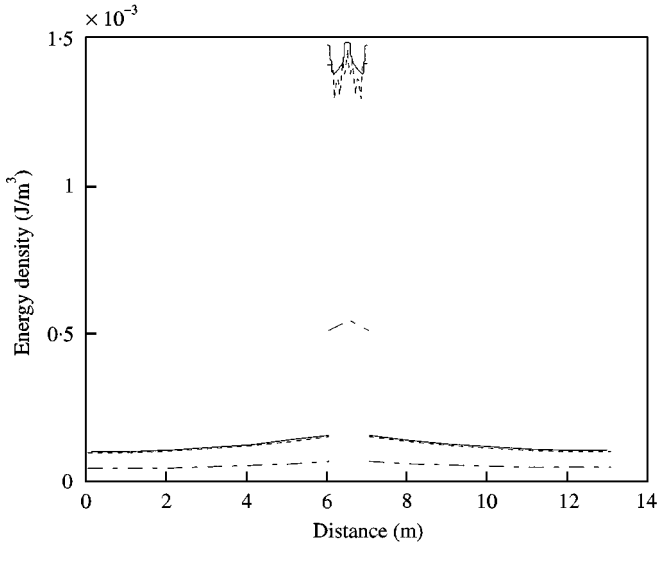

Figure 8. Analytical, hybrid, and EFEA results for the space-averaged energy density in System 2, 495 Hz: ———, analytical; ----, hybrid; - · - · - ·, EFEA.

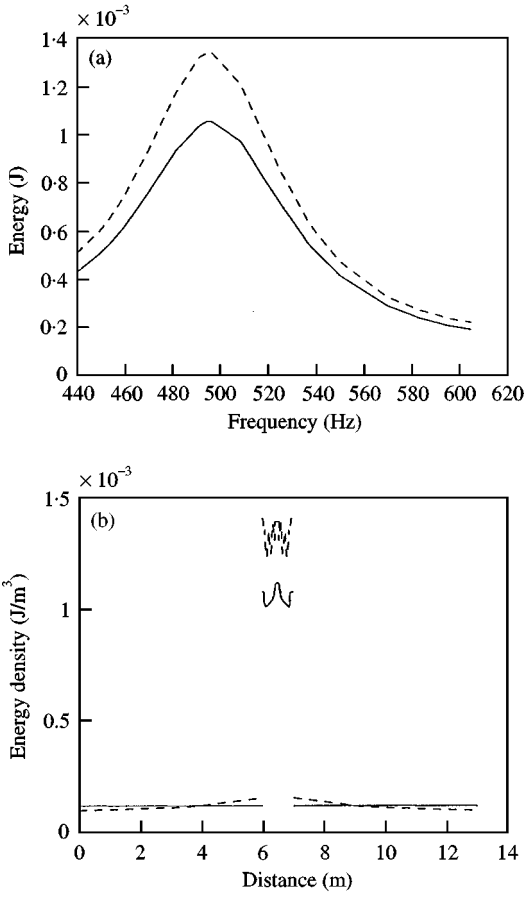

Figure 9. Analytical, and hybrid results for the space-averaged energy density in the semi-infinite solution and System 2: ———, semi-infinite solution; ----, System 2. (a) The short beam, 440–605 Hz; (b) the whole system, 495 Hz.

semi-infinite beam models are used to represent the long beams in the system, the results for the short and long beams will deteriorate. Therefore, approximating the long members as semi-infinite does not provide reliable results even in situations where the long members contain a large number of wavelengths as in the case of System 2 (approximately 16 wavelengths).

4. CONCLUSIONS

The development of a hybrid finite element formulation suitable for mid-frequency vibration simulations of systems with one energy type is presented. The excitation is considered to be applied on a short member. A system of interface equations is developed for the joints between long and short members. The EFEA system of equations for the long members, the FEA system of equations for the short members, and the interface equations are solved simultaneously through an iterative but computationally efficient process. Several systems of co-linear beams are utilized for validation because simple analytical solutions can be readily available. From the results it is evident that the hybrid FEA method

developed in this work captures correctly the energy in the short members, the overall response of the system, the relationship between power flow and stored energy, and the resonant effects of the short members. The hybrid FEA offers a significant improvement over a high frequency solution because it computes accurately the amount of input power for a certain external excitation. The consistently good correlation between the hybrid solution and the analytical results for several configurations and over extended frequency ranges demonstrates the proper development and implementation of the coupling between EFEA and FEA solutions and the overall validity of the hybrid FEA formulation. During the theoretical development no assumptions are made that would prohibit the extension of this work to members with multiple types of waves or to members connected at arbitrary angles.

ACKNOWLEDGMENTS

This research was sponsored by the Automotive Research Center (ARC) established at The University of Michigan, Ann Arbor, by the U.S. Army/Tank-Automotive and Armaments Command (TACOM).

REFERENCES

1. M. A. GOCKEL (editor). 1983 *MSC/NASTRAN Handbook for Dynamic Analysis*. The MacNeal-Schwendler Corporation. Los Angeles, CA.
2. K. J. BATHE 1982 *Finite Element Procedures in Engineering Analysis*. Englewood Cliffs, NJ: Prentice-Hall.
3. K. H. HUEBNER and E. A. THORNTON 1982 *The Finite Element Method for Engineers*. New York: Wiley, second edition.
4. C. B. BURROUGHS, R. W. FISCHER and F. R. KERN 1997 *Journal of the Acoustical Society of America* **101**, 1779–1789. An introduction to statistical energy analysis.
5. C. J. RADCLIFFE and X. L. HUANG 1997 *Journal of Vibration and Acoustics* **119**, 629–634. Putting statistics into the statistical energy analysis of automotive vehicles.
6. R. S. THOMAS, J. PAN, M. J. MOELLER and T. W. NOLAN 1997 *Noise Control Engineering Journal* **45**, 25–34. Implementing and improving statistical energy analysis models using quality technology.
7. J. WOODHOUSE 1991 *Journal of the Acoustical Society of America* **69**, 1695–1709. An approach to the theoretical background of statistical energy analysis applied to structural vibration.
8. R. H. LYON 1975 *Statistical Energy Analysis of Dynamical Systems*: *Theory and Applications*. Cambridge, MA: The MIT Press.
9. O. M. BOUTHIER and R. J. BERNHARD 1995 *Journal of Sound Vibration* **182**, 149–164. Simple models of the energetics of transversely vibrating plates.
10. J. E. HUFF and R. J. BERNHARD 1995 *Proceedings of Inter-Noise* '95, *Newport Beach*, *CA*, *July*, 1221–1226. Prediction of high frequency vibrations in coupled plates using energy finite element.
11. O. M. BOUTHIER 1992 *Ph.D. Dissertation*, *Mechanical Engineering Department*, *Purdue University*. Energetics of vibrating systems.
12. O. M. BOUTHIER and R. J. BERNHARD 1995 *AIAA Journal* **30**, 34–44. Model of space averaged energetics of plates.
13. D. J. NEFSKE and S. H. SUNG 1989 *Journal of Vibration*, *Acoustics*, *Stress and Reliability* **111**, 94–106. Power flow finite element analysis of dynamic systems: basic theory and applications to beams.
14. N. VLAHOPOULOS, X. ZHAO and T. ALLEN 1999 *Journal of Sound and Vibration* **220**, 135–154. An approach for evaluating power transfer coefficients for spor-welded joints in an energy finite element formulation.
15. N. VLAHOPOULOS, L. O. GARZA-RIOS and C. MOLLO 1999 *Journal of Ship Research* **43**, 143–156. Numerical implementation, validation, and marine applications of an energy finite element formulation.

16. B. R. MACE 1993 *Journal of Sound and Vibration* **166**, 429–461. The statistical energy analysis of two continuous one-dimensional subsystems.
17. L. CREMER, M. HECKL and E. E. UNGAR 1973 *Structure Borne Sound*. New York: Springer Verlag.
18. C. R. FREDO 1997 *Journal of Sound and Vibration* **199**, 645–666. A SEA-like approach for the derivation of energy flow coefficients with a finite element model.
19. K. DELANGE, P. SAS and D. VANDEPITTE 1997 *Journal of Vibration and Acoustics* **119**, 293–303. The use of wave-absorbing elements for the evaluation of transmission characteristics of beam junctions.
20. J. A. STEEL and R. J. M. CRAIK 1994 *Journal of Sound and Vibration* **178**, 553–561. Statistical energy analysis of structure-borne sound transmission by finite element methods.
21. C. SIMMONS 1991 *Journal of Sound and Vibration* **144**, 215–227. Structure-borne sound transmission through plate junctions and estimates of SEA coupling loss factors using the finite element method.
22. J. E. MANNING 1990 1990 *Proceedings of International Congress in Air- and Structure-Borne Sound and Vibration, Auburn, AL, March*, 771–778. Calculation of statistical energy analysis parameters using finite element and boundary element models.
23. W. SEEMAN 1996 *Journal of Sound and Vibration* **197**, 571–587. Transmission and reflection coefficients for longitudinal waves obtained by a combination of refined rod theory and FEM.
24. F. THOUVEREZ, M. VIKTOROVITCH and L. JEZEQUAL 1997 *New Advances in Modal Synthesis of Large Structures* (L. Jezequal, editor), 435–444. Rotterdam, The Netherlands: Balkema. A random boundary element formulation for assembled rods and beams in the mid frequency range.
25. L. LU 1990 *Vehicle Noise* (S. H. Sung, K. H. Hsu, R. F. Keltie, editors), *Winter Annual Meeting of the American Society of Mechanical Engineers, Dallas TX*, 9-12. Dynamic substructuring by FEA/SEA.
26. R. S. LANGLEY and P. BREMNER 1999 *Journal of the Acoustical Society of America* **105**, 1657–1671. A hybrid method for the vibration analysis of complex structural-acoustic systems.
27. N. VLAHOPOULOS and X. ZHAO 1999 *AIAA Journal* **37**, 1495–1505. Basic development of hybrid finite element method for mid-frequency structural vibrations.
28. J. S. SUN, C. WANG and Z. H. SUN 1996 *Journal of Sound and Vibration* **189**, 215–229. Power flow between three series coupled oscillators.
29. B. R. MACE 1992 *Journal of Sound and Vibration* **154**, 289–319. Power flow between two continuous one-dimensional subsystems: a wave solution.
30. N. VLAHOPOULOS, C. VILLANCE and R. D. STARK 1998 *Journal of Spacecraft and Rockets* **35**, 355–360. Numerical approach for computing noise-induced vibration from launch environments.
31. N. VLAHOPOULOS, S. T. RAVEENDRA, C. VALLANCE and S. MESSER 1999 *Finite Elements in Analysis and Design* **32**, 257–277. Numerical implementation and applications of a coupling algorithm for structural-acoustic models with unequal discretization and partially interfacing surfaces.
32. P. CHO 1993 *Ph.D. Dissertation, Mechanical Engineering Department, Purdue University*. Energy flow analysis of coupled structures.
33. B. R. MACE 1992 *Journal of Sound and Vibration* **159**, 305–325. Power flow between two coupled beams.

APPENDIX A: ANALYTICAL SOLUTION

The analytical solution for systems of co-linear beams is computed by a MATLAB code. First the displacement solutions for each beam are considered:

$$W_l(x_l, t) = (A_l e^{-ik_l x_l} + B_l e^{-k_l x_l} + C_l e^{ik_l x_l} + D_l e^{k_l x_l}) e^{i\omega t} \quad \text{for a long member,} \tag{A.1}$$

$$W_s(x_s, t) = (A_s e^{-ik_s x_s} + B_s e^{-k_s x_s} + C_s e^{ik_s x_s} + D_s e^{k_s x_s}) e^{i\omega t} \quad \text{for a short member,} \tag{A.2}$$

where subscripts "l" and "s" are associated with the long and short members respectively, $W_l(x_l, t)$ is the analytical displacement solution of a long member (function of x_l and t), A_l the amplitude of the right travelling farfield wave, B_l the amplitude of the right travelling

near-field wave, C_l the amplitude of the left travelling far field wave, D_l the amplitude of the left travelling nearfield wave, k_l the complex flexural wave number of the long member, ω the radial frequency, and $W_s(x_s, t)$, A_s, B_s, C_s, D_s, k_s are the corresponding expressions for a short member. A separate reference system is utilized for each member. The origin is positioned at the left end of each member. The power flow and energy density in the long and the short members are expressed in terms of the corresponding analytical displacement solutions.

Power flow in a beam is transmitted by shear and moment mechanisms. The time-averaged power associated with the shear force and the moment is

$$\langle q_l \rangle = \frac{1}{2} E_l I_l Re \left\{ \frac{\partial^3 W_l}{\partial x_l^3} \left(\frac{\partial W_l}{\partial t} \right)^* - \frac{\partial^2 W_l}{\partial x_l^2} \left(\frac{\partial^2 W_l}{\partial x_l \partial t} \right)^* \right\} \quad \text{for a long member,} \tag{A.3}$$

$$\langle q_s \rangle = \frac{1}{2} E_s I_s Re \left\{ \frac{\partial^3 W_s}{\partial x_s^3} \left(\frac{\partial W_s}{\partial t} \right)^* - \frac{\partial^2 W_s}{\partial x_s^2} \left(\frac{\partial^2 W_s}{\partial x_s \partial t} \right)^* \right\} \quad \text{for a short member.} \tag{A.4}$$

The total energy density in a transversely vibrating beam is the sum of its potential energy density V and kinetic energy density T. The time-average total energy density solutions for the long and the short members are

$$\langle e_l \rangle = \frac{1}{4} \frac{E_l I_l}{S_l} \left\{ \frac{\partial^2 W_l}{\partial x_l^2} \left(\frac{\partial^2 W_l}{\partial x_l^2} \right)^* \right\} + \frac{1}{4} \rho_l \left\{ \frac{\partial W_l}{\partial t} \left(\frac{\partial W_l}{\partial t} \right)^* \right\} \quad \text{for a long member,} \tag{A.5}$$

$$\langle e_s \rangle = \frac{1}{4} \frac{E_s I_s}{S_s} \left\{ \frac{\partial^2 W_s}{\partial x_s^2} \left(\frac{\partial^2 W_s}{\partial x_s^2} \right)^* \right\} + \frac{1}{4} \rho_s \left\{ \frac{\partial W_s}{\partial t} \left(\frac{\partial W_s}{\partial t} \right)^* \right\} \quad \text{for a short member.} \tag{A.6}$$

Substitution of the displacement solution (equations (A.1) and (A.2)) into equations (A.5) and (A.6) allows to express the time-averaged energy density as

$$\begin{aligned} \langle e_l \rangle = \frac{1}{4} \frac{E_l I_l}{S_l} |k_l^2|^2 \times & (- A_l e^{-ik_l x_l} + B_l e^{-k_l x_l} - C_l e^{ik_l x_l} + D_l e^{k_l x_l}) \\ & \times (- A_l e^{-ik_l x_l} + B_l e^{-k_l x_l} - C_l e^{ik_l x_l} + D_l e^{k_l x_l})^* + \tfrac{1}{4} \rho_l \omega^2 \\ & \times (A_l e^{-ik_l x_l} + B_l e^{-k_l x_l} + C_l e^{ik_l x_l} + D_l e^{k_l x_l}) \\ & \times (A_l e^{-ik_l x_l} + B_l e^{-k_l x_l} + C_l e^{ik_l x_l} + D_l e^{k_l x_l})^*, \end{aligned} \tag{A.7}$$

$$\begin{aligned} \langle e_s \rangle = \frac{1}{4} \frac{E_s I_s}{S_s} |k_s^2|^2 \times & (- A_s e^{-ik_s x_s} + B_s e^{-k_s x_s} - C_s e^{ik_s x_s} + D_s e^{k_s x_s}) \\ & \times (- A_s e^{-ik_s x_s} + B_s e^{-k_s x_s} - C_s e^{ik_s x_s} + D_s e^{k_s x_s})^* + \tfrac{1}{4} \rho_s \omega^2 \\ & \times (A_s e^{-ik_s x_s} + B_s e^{-k_s x_s} + C_s e^{ik_s x_s} + D_s e^{k_s x_s}) \\ & \times (A_s e^{-ik_s x_s} + B_s e^{-k_s x_s} + C_s e^{ik_s x_s} + D_s e^{k_s x_s})^*. \end{aligned} \tag{A.8}$$

Finally, the energy density $\langle e_l \rangle$ and $\langle e_s \rangle$ are spaced-averaged over one wavelength to obtain the analytical expressions for the time- and space-averaged energy density $\langle \underline{e_l} \rangle$ and $\langle \underline{e_s} \rangle$ in the long and the short members respectively.